Oxygenation and chlorination of aromatic hydrocarbons with hydrochloric acid photosensitized by 9-mesityl-10-methylacridinium under visible light irradiation

Kei Ohkubo · Kentaro Mizushima · Shunichi Fukuzumi

Abstract Efficient photocatalytic oxygenation of toluene occurs under visible light irradiation of 9-mesityl-10-methylacridinium (Acr$^+$–Mes) in oxygen-saturated acetonitrile containing toluene and aqueous hydrochloric acid with a xenon lamp for 15 h. The oxygenated products, benzoic acid (70 %) and benzaldehyde (30 %), were formed after the photoirradiation. The photocatalytic reaction is initiated by intramolecular photoinduced electron transfer from the mesitylene moiety to the singlet excited state of the Acr$^+$ moiety of Acr$^+$–Mes, which affords the electron-transfer state, Acr$^\bullet$–Mes$^{\bullet+}$. The Mes$^{\bullet+}$ moiety can oxidize chloride ion (Cl$^-$) by electron transfer to produce chlorine radical (Cl$^\bullet$), whereas the Acr$^\bullet$ moiety can reduce O$_2$ to O$_2^{\bullet-}$. The Cl$^\bullet$ radical produced abstracts a hydrogen from toluene to afford benzyl radical in competition with the bimolecular radical coupling of Cl$^\bullet$. The benzyl radical reacts with O$_2$ rapidly to afford the peroxyl radical, leading to the oxygenated product, benzaldehyde. Benzaldehyde is readily further photooxygenated to yield benzoic acid with Acr$^\bullet$–Mes$^{\bullet+}$. In the case of an aromatic compound with electron-donating substituents, 1,3,5-trimethoxybenzene, photocatalytic chlorination occurred efficiently under the same photoirradiation conditions to yield a monochloro-substituted compound, 2,4,6-trimethoxychlorobenzene.

Keywords Electron transfer · Oxygenation · Chlorination · Radical cation · Photocatalysis

K. Ohkubo (✉) · K. Mizushima · S. Fukuzumi (✉)
Department of Material and Life Science, Graduate School of Engineering, Osaka University and ALCA (JST), Suita, Osaka 565-0871, Japan
e-mail: ookubo@chem.eng.osaka-u.ac.jp

S. Fukuzumi
e-mail: fukuzumi@chem.eng.osaka-u.ac.jp

S. Fukuzumi
Department of Bioinspired Science, Ewha Womans University, Seoul 120-750, Korea

Introduction

Oxygenation and halogenations of hydrocarbons are important and fundamental chemical reactions, providing key precursors for various transformations. Although there have been many reports on oxygenation and halogenation of hydrocarbon, it is highly desired to develop more effective and environmentally benign methods, because the current methodology requires drastic conditions or excessive use of heavy metals as oxidants [1–4]. With this background in mind, it has recently been reported that catalytic oxidation processes with hydrogen peroxide or molecular oxygen can diminish waste [5–11]. From a "green chemistry" perspective, the best candidate for an oxidant would be molecular oxygen because of its abundant availability and non-toxicity [12–16].

Radical species which can react with molecular oxygen can be readily generated by photoinduced electron-transfer reactions [17–25]. The radical cation of ring-substituted toluenes readily deprotonates to give the corresponding benzyl radicals, which can react with molecular oxygen directly to produce the benzyl peroxyl radicals, leading to the final oxygenated products [26–30]. The key step in such reactions is electron-transfer oxidation of substrates. A main problem in such a case is that the one-electron reduction potentials of the excited states of photosensitizers should be higher than the one-electron oxidation potentials of substrates, because the photocatalytic reactions are initiated by the electron-transfer oxidation of substrates [26].

We have reported that the photoexcitation of 9-mesityl-10-methylacridinium (Acr^+–Mes) results in ultrafast electron transfer from the Mes moiety to the singlet excited state of the Acr^+ moiety to form the electron-transfer state ($Acr^{\bullet}$–$Mes^{\bullet+}$), which has an extremely long lifetime (e.g., 2 h at 203 K) and a high energy (2.37 eV). The electron-transfer state ($Acr^{\bullet}$–$Mes^{\bullet+}$) has a strong oxidizing agent with the $Mes^{\bullet+}$ moiety as well as a strong reducing agent with the $Acr^{\bullet}$ moiety [31, 32]. In such a case, Acr^+–Mes acts as an efficient electron-transfer photocatalyst for highly selective oxygenation of substrates. However, substrates that can be oxidized by $Acr^{\bullet}$–$Mes^{\bullet+}$ via electron transfer have been limited to those with the lower one-electron oxidation potentials than the one-electron reduction potential of $Acr^{\bullet}$–$Mes^{\bullet+}$. Thus, the use of Acr^+–Mes as an efficient electron-transfer photocatalyst has yet to be expanded to photooxidation of toluene with O_2 to yield benzoic acid because one-electron reduction potential of $Acr^{\bullet}$–$Mes^{\bullet+}$ ($E_{red} = + 2.06$ V vs. SCE) [33] is lower than the oxidation potential of toluene ($E_{ox} = + 2.20$ V) [34].

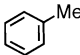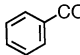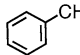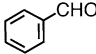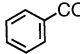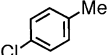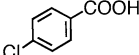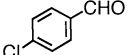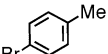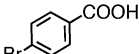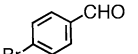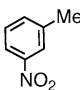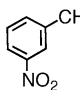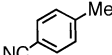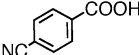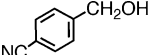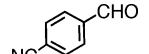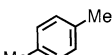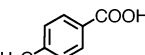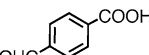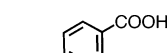Herein, we expand the scope of the use of Acr^+–Mes as an efficient electron-transfer photocatalyst for oxidation of organic compounds with O_2 other than oxygenation reactions by examining photocatalytic oxygenation of toluene with O_2 and hydrochloric acid. We have also found the photocatalytic chlorination of methoxy-subsituted benzenes with HCl and O_2 by Acr^+–Mes, where the radical cation of substrate acts as a strong electrophile to efficiently react with a nuclephile, Cl^- to yield the chlorinated product. The photocatalytic mechanism is clarified by detecting radical intermediates involved in the photocatalytic reactions with use of nanosecond laser flash photolysis.

Experimental

Materials

9-Mesityl-10-methylacridinium perchlorate (Acr^+–Mes ClO_4^-) and substrates shown in Table 1 except for benzaldehyde and toluene were obtained from Tokyo Chemical Industry. Hydrochloric acid (30 %) and toluene, benzaldehyde, sodium iodide and hydrogen peroxide were obtained from Wako Pure Chemicals and used without further purification except for benzaldehyde. Benzaldehyde was washed with aqueous Na_2CO_3 solution in three times and distilled to remove the contaminants. Acetonitrile (MeCN) was of spectral grade, obtained commercially, and used without further purification.

Table 1 Products and quantum yields for photocatalytic oxygenation of aromatic hydrocarbons by O_2 with HCl and Acr^+–Mes in O_2-saturated MeCN (conditions: [substrate] = 10 mM, [Acr^+-Mes ClO_4^-] = 1.0 mM, HCl = 1.0 mM)

Substrate	Carboxylic acid	Yield (%)	Aldehyde	Yield (%)	Conv. (%)	Time (h)	Φᵃ (%)
Me (toluene)	COOH (benzoic acid)	87	CHO (benzaldehyde)	13	100	13	0.44
CHO (benzaldehyde)	COOH (benzoic acid)	95			95	5	1.13ᵇ
Cl–C6H4–Me	Cl–C6H4–COOH	95	Cl–C6H4–CHO	5	100	12	0.63
Br–C6H4–Me	Br–C6H4–COOH	96	Br–C6H4–CHO	4	100	12	0.56
NO2–C6H4–Me			NO2–C6H4–CHO	20	20	10	–
NC–C6H4–Me	NC–C6H4–COOH	14	NC–C6H4–CH2OH	7	44	10	0.01
			NC–C6H4–CHO	23			
Me–C6H4–Me	H3C–C6H4–COOH	38	OHC–C6H4–COOH	13	100	13	–
	HOOC–C6H4–COOH	16					

Photoirradiation by use of a xenon lamp attached with a color glass filter ($\lambda < 420$ nm)

ᵃ Φ was determined from the amount of the formation of benzaldehyde

ᵇ Φ was determined from the amount of benzoic acid

Reaction procedures

The photocatalytic oxygenation of toluene with O_2 in the presence of HCl was carried out by the following procedure. Typically, an MeCN solution (0.60 mL) containing Acr^+–Mes ClO_4^- (0.25 mg, 6.0×10^{-7} mol) and toluene (0.64 mg, 6.0×10^{-6} mol) in an NMR tube with a rubber septum was saturated with oxygen by bubbling oxygen through a Teflon tube for 5 min. The solution was then irradiated with a 500-W xenon lamp (Ushio Optical ModelX SX-UID 500XAMQ) through a color filter glass (Asahi Techno Glass Y43) transmitting $\lambda > 430$ nm at 278 K. After photoirradiation for 13 h, the corresponding benzaldehyde and benzoic acid were identified by comparison with those of an authentic samples in the GC retention time and the GC/MS spectra (Shimadzu QP-5000), and also by ^{1}H NMR spectra. Benzaldehyde: ^{1}H NMR (300 MHz, CD_3CN, ppm): δ 10.0 (s, 1H), 7.89 (d, $J = 6.9$ Hz, 2H), 7.68 (t, $J = 7.3$ Hz, 1H), 7.58 (t, $J = 7.9$ Hz, 2H). Benzoic acid: ^{1}H NMR (300 MHz, CD_3CN, ppm) δ 8.00 (d, $J = 7.8$ Hz, 2H), 7.62 (m, 1H), 7.48 (m, 2H).

The photocatalytic chlorination of 1,3,5-trimethoxybenzene (TMB) by O_2 with Acr^+–Mes ClO_4^- in the presence of HCl was carried out as follows. Typically, an acetonitrile-d_3 solution (0.60 mL) containing Acr^+–Mes (0.050 mg, 1.2×10^{-7} mol) and TMB (0.40 mg, 2.4×10^{-6} mol) in an NMR tube with a rubber septum was saturated with oxygen by bubbling oxygen gas through a stainless steel needle for 5 min. The solution was then irradiated with a 500-W xenon lamp through a color filter glass transmitting ($\lambda < 430$ nm) at 278 K. After photoirradiation for 6 h, 2,4,6-trimethoxychlorobenzene was identified by comparing the ^{1}H NMR spectrum in comparison with that of an authentic sample. 2,4,6-Trimethoxychlorobenzene: ^{1}H NMR (300 MHz, CD_3CN, ppm) δ 6.27 (s, 2H), 3.82 (s, 3H), 3.78 (s, 6H).

The amount of H_2O_2 was determined by titration by iodide ion as follows [35–37]. An O_2-saturated MeCN solution (0.60 mL) of Acr^+–Mes (1.0×10^{-3} M) and toluene (1.0×10^{-2} M) was photoirradiated and the photoirradiated product mixture was diluted with an MeCN solution containing excess amount of NaI. The amount of I_3^- formed was then determined from the UV–Vis spectrum ($\lambda_{max} = 361$ nm, $\lambda = 2.5 \times 10^4$ M^{-1} cm^{-1}) [36, 37].

Quantum yield determinations

Potassium trisoxalatoferrate(III) as a standard actinometer [38] was used to determine the quantum yield of the photocatalytic oxygenation of toluene with O_2 in the presence of Acr^+–Mes. A square quartz cuvette (10 mm i.d.), which contained a degassed MeCN solution (3.0 mL) of Acr^+–Mes ClO_4^- (1.0×10^{-3} M) and toluene (0–0.25 M), was irradiated with steady-state monochromatized light ($\lambda = 430$ nm) from a Shimadzu RF-5300PC fluorescence spectrophotometer. Under the conditions of actinometry experiments, the actinometer and Acr^+–Mes absorbed essentially all the incident light of $\lambda = 430$ nm. The light intensity of monochromatized light of $\lambda = 430$ nm was determined to be 9.9×10^{-7} einstein s^{-1}. In addition, a square quartz cuvette (10 mm i.d.), which contained a

degassed MeCN solution (3.0 mL) of Acr^+–Mes (2.0×10^{-4} M) and toluene (0–0.2 M), was irradiated with monochromatized laser flash ($\lambda = 430$ nm) from Nd:YAG laser (Continuum, SLII-10, 4-6 ns fwhm). The light intensity of monochromatized light of $\lambda = 430$ nm was determined to be 8.6×10^{-8} einstein/pulse. The photochemical reaction was monitored using a Hewlett Packard 8453 diode-array spectrophotometer.

Laser flash photolysis measurements

Measurements of transient absorption spectra in the photochemical reactions of Acr^+–Mes with toluene were performed according to the following procedure. A degassed MeCN solution containing Acr^+–Mes ClO_4^- (2.0×10^{-4} M), toluene (1.5×10^{-4} M) and HCl (2.0×10^{-4} M) was excited by Nd:YAG laser (Continuum, SLII-10, 4–6 ns fwhm) at 430 nm. Time courses of the transient absorption spectra were measured by using a continuous xenon lamp (150 W) and an InGaAs-PIN photodiode (Hamamatsu 2949) as a probe light and a detector, respectively. The output from the photodiodes and a photomultiplier tube was recorded with a digitizing oscilloscope (Tektronix, TDS3032, 300 MHz). The transient spectra were recorded using fresh solutions in each laser excitation. All experiments were performed at 298 K.

Results and discussion

Photocatalytic oxygenation of toluene with O_2

Visible light irradiation ($\lambda > 430$ nm) of the absorption band of 9-mesityl-10-methylacridinium perchlorate (Acr^+–Mes ClO_4^-; 5.0×10^{-3} M) in an O_2-saturated acetonitrile (MeCN) solution containing toluene (1.5×10^{-2} M) for 5 h by using a 500-W xenon lamp resulted in the formation of an oxygenated product in very low yield, i.e., benzaldehyde in 2 % yield (Eq. 1).

$$2 \, \text{PhCH}_3 + 3 \, O_2 \xrightarrow{h\nu} 2 \, \text{PhCHO} + 2 \, H_2O_2$$

(1)
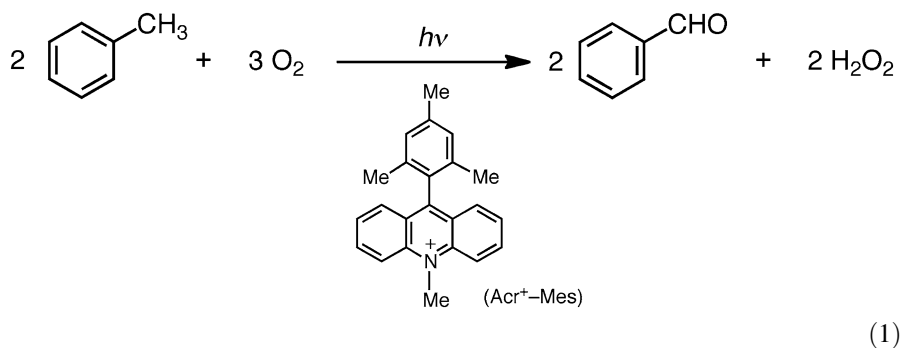
In the presence of HCl under the same irradiation conditions, toluene was consumed with a concomitant formation of benzaldehyde (60 %), benzoic acid
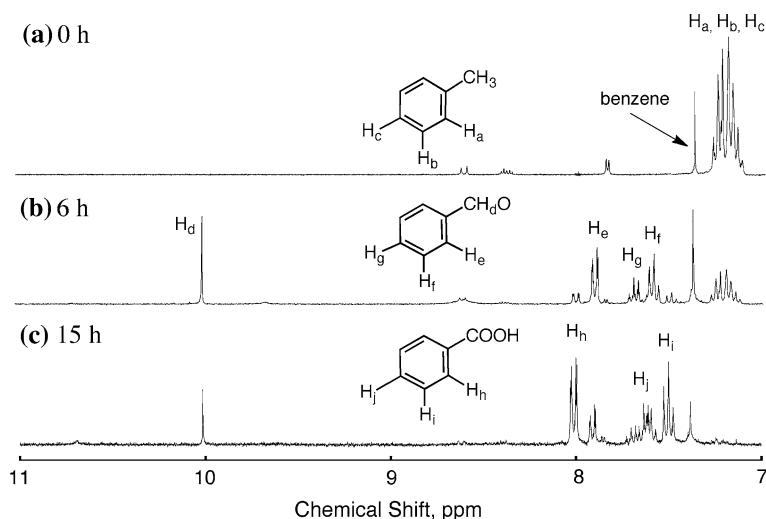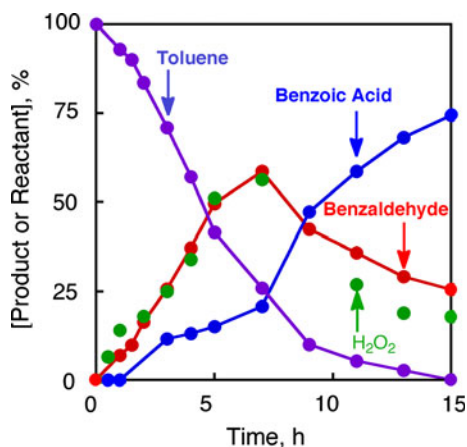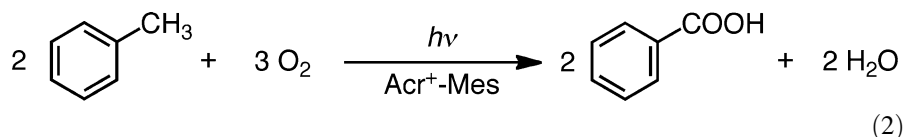
Fig. 1 ^{1}H NMR spectra of oxygen-saturated CD$_3$CN solutions containing Acr$^+$–Mes ClO$_4^-$ (1.0×10^{-3} M), toluene (1.0×10^{-2} M) and HCl (1.0×10^{-3} M) **a** before and after photoirradiation for **b** 6 h and **c** 15 h. Benzene was used as an internal standard

(20 %), and hydrogen peroxide (H$_2$O$_2$, 60 %) after 7 h photoirradiation (Fig. 1). The yields of oxygenated products and H$_2$O$_2$ were determined by ^{1}H NMR and iodemetry measurements, respectively. The time course in photocatalytic oxygenation is shown in Fig. 2. Prolonged photoirradiation afforded benzoic acid with the consumption of benzaldehyde. The yields of final products after 15 h photoirradiation were 30 % for benzaldehyde, 70 % for benzoic acid and 20 % for H$_2$O$_2$. The total stoichiometry for oxygenation of toluene to benzoic acid is given by Eq. 2. The photocatalytic turnover

Fig. 2 Irradiation time profiles of product formation and reactant consumption in Acr$^+$–Mes catalyzed photooxygenation of toluene (1.0×10^{-2} M) in O$_2$-saturated MeCN (0.6 mL) at 298 K; Acr$^+$–Mes ClO$_4^-$: 1.0×10^{-3} M, HCl: 1.0×10^{-3} M

$$2 \underset{}{\text{C}_6\text{H}_5\text{CH}_3} + 3\ \text{O}_2 \xrightarrow[\text{Acr}^+\text{-Mes}]{hv} 2\ \underset{}{\text{C}_6\text{H}_5\text{COOH}} + 2\ \text{H}_2\text{O} \tag{2}$$

number was determined to be 50. No oxygenation of the mesitylene moiety of Acr$^+$–Mes occurred under photoirradiation in the presence of substrate and HCl because the electron-transfer state of Acr$^+$–Mes is efficiently quenched by the large excess of HCl to give the ground state of Acr$^+$–Mes [39]. It was also confirmed that no chlorinated substrate was observed under the present experimental conditions.

When Acr$^+$–Mes was replaced by 9-phenyl-10-methylacridinium (Acr$^+$–Ph), the photooxygenated products were also obtained as 8 % yield of benzoic acid after 15 h photoirradiation. The photocatalytic reactivity of Acr$^+$–Ph is significantly lower than the case of Acr$^+$–Mes. In contrast to the case of Acr$^+$–Mes, the photocatalytic oxygenation of toluene with O$_2$ in the presence of Acr$^+$–Ph proceeds via electron transfer from Cl$^-$ to Acr$^+$–Ph. However, the lifetime of the singlet excited state of Acr$^+$–Ph ($\lambda = 1.5$ ns in MeCN) [26] is much shorter than that of the electron-transfer state of Acr$^+$–Mes [31]. A high concentration of substrate is needed to quench the short-lived singlet excited state of Acr$^+$–Ph.

When Acr$^+$–Mes was replaced by 9-mesityl-2,7,10-trimethylacridinium (Me$_2$Acr$^+$–Mes) which has a stronger reducing ability of the electron-transfer state than Acr$^+$–Mes [33], the yield of benzoic acid was 13 % in the Me$_2$Acr$^+$–Mes catalyzed photooxygenatyion. The low catalytic reactivity of Me$_2$Acr$^+$–Mes is attributed to the lower quantum yield of the electron-transfer state of Me$_2$Acr$^+$–Mes (60 %) as compared to Acr$^+$–Mes (98 %) [31, 33]. When benzaldehyde was used as a starting material, the photocatalytic oxygenation in MeCN also occurred to yield benzoic acid. The yield of benzoic acid was 70 % after 8 h photoirradiation as shown in Fig. 3. The catalytic reactivity was only slightly increased by addition of

Fig. 3 Irradiation time profiles of the Acr$^+$–Mes—photosensitized oxygenation of benzaldehyde (1.0×10^{-2} M) in oxygen-saturated MeCN (0.6 mL) containing Acr$^+$–Mes ClO$_4^-$ (1.0×10^{-3} M), HCl (1.0×10^{-3} M) and H$_2$O$_2$ (0 M and 1.0 mM) at 298 K
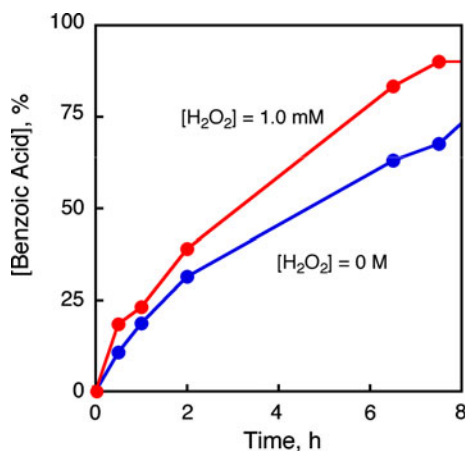
H_2O_2 (1.0 mM) as shown in Fig. 3. Thus, H_2O_2 does not play a major role in the photocatalytic oxygenation of benzaldehyde to benzoic acid in this catalytic system.

The quantum yields (Φ) of formation of the photooxygenated product under photoirradiation ($\lambda > 430$ nm) were determined by following appearance of ^1H NMR peaks due to toluene. The dependence of Φ value on concentration of toluene in the Acr^+–Mes catalyzed photooxygenation of toluene in O_2-saturated MeCN is shown in Fig. 4a. The Φ value increases with increasing concentration of toluene ([Toluene]) to reach a constant value. Such a saturated dependence of Φ on the [Toluene] is expressed by Eq. 3, where K_{obs} is defined as $k_2 k_1^{-1} [Cl^\bullet]^{-1}$. k_1 is the

$$\Phi = \Phi_\infty K_{obs}[Toluene]/(1 + K_{obs}[Toluene]) \qquad (3)$$

rate constant of back electron transfer from Cl^- to $Acr^\bullet$–Mes, and k_2 is the rate constant of hydrogen abstraction of toluene by $Cl^\bullet$ (Scheme 1). Equation 3 is rewritten as Eq. 4. The saturated dependence of Φ on [Toluene] was converted

$$\Phi^{-1} = \Phi_\infty^{-1}\left[1 + (K_{obs}[Toluene])^{-1}\right] \qquad (4)$$

to a linear plot of Φ^{-1} versus $[Toluene]^{-1}$ as shown in Fig. 4b. From the slope and intercept, the Φ_∞ and K_{obs} values were determined to be 2.6×10^{-2} and 2.7×10^2 M^{-1}, respectively.

Table 1 shows the yields and Φ values of the photocatalytic oxygenation of a series of substrates including those with electron-withdrawing groups. Each reaction proceeds in high conversion to yield the corresponding carboxylic acid and aldehyde. In the case of p-xylene as a substrate, telephthalic acid was obtained in 16 % yield.

In order to elucidate the photocatalytic oxygenation mechanism, laser flash photolysis was performed to detect the intermediates. Nanosecond laser excitation at 430 nm of a degassed MeCN solution of Acr^+–Mes resulted in formation of the
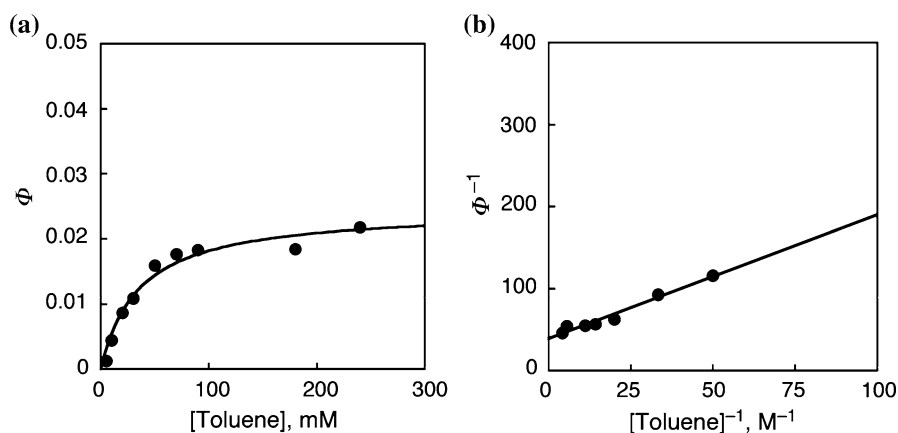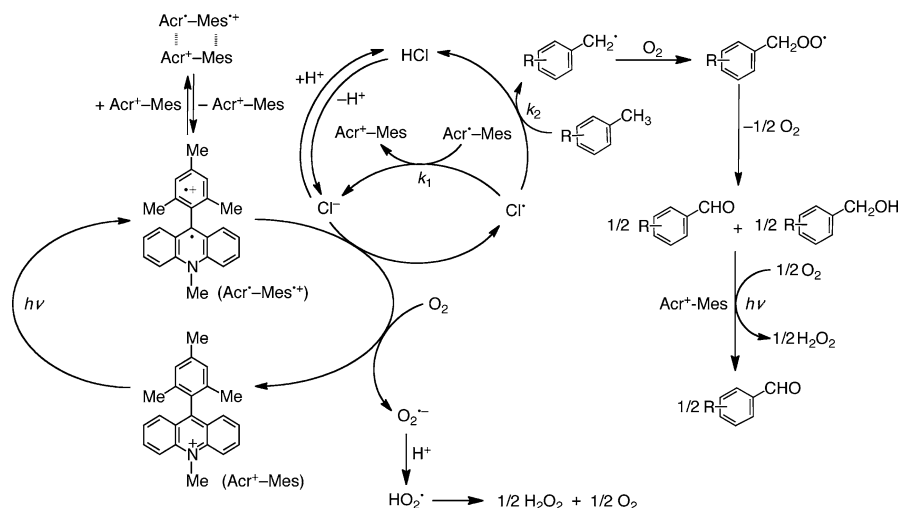

Fig. 4 **a** Dependence of quantum yield of benzaldehyde on [Toluene] for the photocatalytic reaction O_2-saturated MeCN containing Acr^+–Mes ClO_4^- (1.0 mM), toluene (0.5–240 mM) and HCl (1.0 mM) after the photoirradiation (80 min, $\lambda > 430$ nm). **b** Plot of Φ^{-1} versus $[Toluene]^{-1}$

Scheme 1 Proposed reaction mechanism for photooxygenation of toluene derivatives catalyzed by Acr$^+$–Mes and HCl

electron-transfer state (Acr$^\bullet$–Mes$^{\bullet+}$) via photoinduced electron transfer from the Mes moiety to the singlet excited state of the Acr$^+$ moiety as shown in Fig. 5. The quantum yield for the formation of Acr$^\bullet$–Mes$^{\bullet+}$ by intramolecular photoinduced electron transfer has been previously determined to be nearly quantitative (98 %) [31].

The absorption band at 500 nm is due to the Acr$^\bullet$ moiety overlapped with the Mes$^{\bullet+}$ moiety [31, 32]. The absorption band at 500 nm was previously assigned to the triplet excited state of the Acr$^+$ moiety [40–44]. However, the absorption band at 500 nm is accompanied by a near-IR absorption, which was clearly assigned to the π-dimer radical cation formed between the electron-transfer state (Acr$^\bullet$–Mes$^{\bullet+}$) and the ground state of Acr$^+$–Mes [45, 46]. A similar near-IR absorption was observed for the π-dimer radical cation formed between the electron-transfer state of

Fig. 5 Transient absorption spectrum of electron-transfer state of Acr$^+$–Mes in deaerated MeCN without HCl taken at 6 μs after nanosecond laser excitation ($\lambda = 430$ nm)
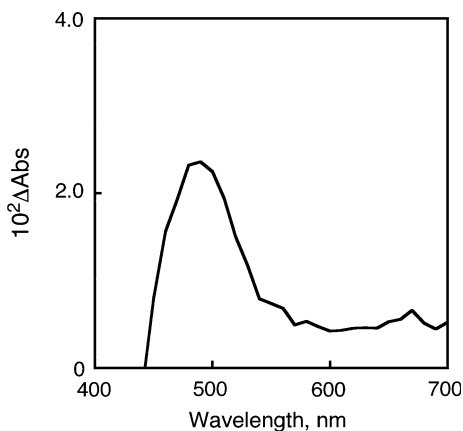
2-phenyl-4-(1-naphthyl)quinolinium and the ground state [47, 48]. Thus, the absorption band at 500 nm does not originate from the triplet excited state but the electron-transfer state. It should be pointed out that the energy of acridinium triplet was mistakenly reported to be 1.96 eV, which is lower than the electron-transfer state (Acr$^\bullet$–Mes$^{\bullet+}$) [41, 42]. However, the reported low triplet energy value corresponds to the strong phosphorescence of the corresponding acridine, which remains as impurity according to the reported synthetic method [41, 42]. It is well known that acridine derivatives exhibit phosphorescence with the same energy of 1.96 eV as the mistakenly reported value for the acridinium ion [49]. It is also well known that the triplet energy of acridinium ion is significantly higher than that of the corresponding acridine [50, 51]. It should be emphasized that the electron-transfer state (Acr$^\bullet$–Mes$^{\bullet+}$) has not only strong oxidizing ability but also strong reducing ability, both of which have been utilized a variety of photoinduced redox processes [52–69].

The decay rate constant of the transient absorption band due to the Mes$^{\bullet+}$ moiety of Acr$^\bullet$–Mes$^{\bullet+}$ increases with increasing concentration of HCl as shown in Fig. 6. The formation rate obeys pseudo-first-order kinetics, and the pseudo-first-order rate constant increases linearly with increasing concentration of HCl (Fig. 6). The second-order rate constant of electron transfer from Cl$^-$ to Acr$^\bullet$–Mes$^{\bullet+}$ was determined from the slope of the linear plot in Fig. 6 to be 9.5×10^8 M^{-1} s^{-1}. Because the one-electron reduction potential of Acr$^\bullet$–Mes$^{\bullet+}$ ($E_{red} = +2.06$ V vs. SCE) [33] is more positive than the one-electron oxidation potential of Cl$^-$ ($E_{ox} = +1.15$ V vs. SCE) [39], electron transfer from Cl$^-$ to the Mes$^{\bullet+}$ moiety in Acr$^\bullet$–Mes$^{\bullet+}$ is energetically quite feasible. Thus, in the presence of HCl, electron transfer from Cl$^-$ to the Mes$^{\bullet+}$ moiety occurs to produce Cl$^\bullet$ and Acr$^\bullet$–Mes [39]. This indicates clearly that Cl$^\bullet$ is formed by electron transfer from Cl$^-$ to Acr$^\bullet$–Mes$^{\bullet+}$ rather than by direct photoinduced electron transfer from Cl$^-$ to the singlet excited state of the Acr$^+$ moiety in Acr$^+$–Mes.

On the other hand, the rate constant of electron transfer from toluene to Acr$^\bullet$–Mes$^{\bullet+}$ was determined to be 2.0×10^6 M^{-1} s^{-1} (Fig. 6), which is significantly smaller than the rate of electron transfer from Cl$^-$ to Acr$^\bullet$–Mes$^{\bullet+}$. Electron transfer

Fig. 6 Plots of k_{decay} versus [Toluene or HCl] for the electron-transfer oxidation of toluene or HCl with Acr$^\bullet$–Mes$^{\bullet+}$ in deaerated MeCN at 298 K
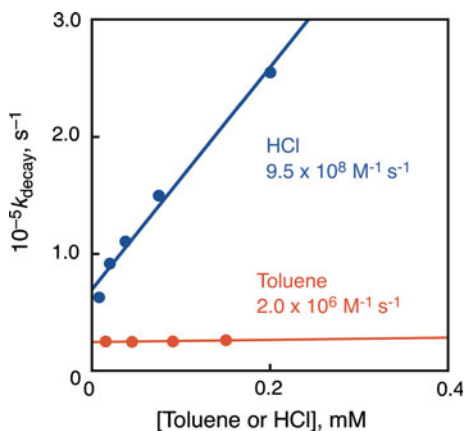
oxidation of toluene with $Acr^\bullet–Mes^{\bullet+}$ is energetically unfavorable, because the one-electron oxidation potential of toluene ($E_{ox} = +2.20$ V vs. SCE) [34] is more positive than the reduction potential of the $Mes^{\bullet+}$ moiety ($+2.06$ V) of $Acr^\bullet–Mes^{\bullet+}$.

The photocatalytic mechanism involving the radical intermediates detected in this study is shown in Scheme 1. Photoexcitation of $Acr^+–Mes$ gives the long-lived electron-transfer state ($Acr^\bullet–Mes^{\bullet+}$) by intramolecular electron transfer from the mesitylene moiety to the acridinium moiety that has strong reducing and oxidizing abilities ($E_{red} = +2.06$ V, $E_{ox} = –0.57$ V vs. SCE) [33]. The electron-transfer state is stabilized as the π-dimer radical cation composed of $Acr^\bullet–Mes^{\bullet+}$ and the ground state of $Acr^+–Mes$ (Scheme 1) [45, 46]. The $Acr^\bullet$ and $Mes^{\bullet+}$ moieties can reduce and oxidize O_2 and Cl^- to give superoxide anion ($O_2^{\bullet-}$) and $Cl^\bullet$, respectively [33, 39]. A hydrogen of the methyl group of toluene is abstracted by $Cl^\bullet$ to afford benzyl radical. This is followed by rapid O_2 addition to afford the peroxyl radical, leading to benzaldehyde and benzyl alcohol via the disproportionation. Benzyl alcohol is readily further oxygenated to yield benzaldehyde with $Acr^\bullet–Mes^{\bullet+}$. On the other hand, $O_2^{\bullet-}$ disproportionates with proton to yield H_2O_2 and O_2 (Scheme 1) [33]. The further oxygenation of benzaldehyde photosensitized by $Acr^+–Mes$ with HCl occurs to yield benzoic acid via abstraction of a hydrogen from the formyl group of benzaldehyde by $Cl^\bullet$.
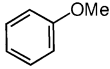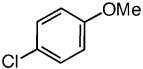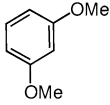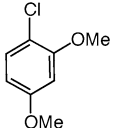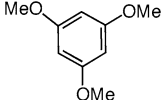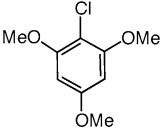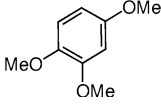
Photocatalytic chlorination of trimethoxybenzene
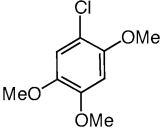
No photooxygenation of TMB occurred, because the hydrogen abstraction from TMB by $Cl^\bullet$ is difficult due to the strong C–H bond of the methoxy group. However, aerobic photocatalytic aromatic chlorination of TMB occurs with $Acr^+–Mes$ and HCl. Visible light irradiation of the absorption band ($\lambda > 430$ nm) of $Acr^+–Mes$ (5.0×10^{-3} M) in an O_2-saturated MeCN solution of TMB containing HCl (6.0×10^{-2} M) resulted in the formation of a chlorinated product, 2,4,5-trimethoxychlorobenzene. The overall stoichiometry of the photocatalytic reaction is given by Eq. 5

$$\text{(5)}$$
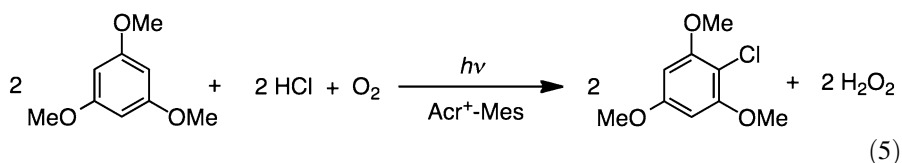
The yield of 2,4,6-trimethoxychlorobenzene and H_2O_2 was determined to be 58 % and 46 % by the ^{1}H NMR and iodometry measurements, respectively (see the "Experimental" section). The photocatalytic chlorination of other methoxybenzene derivatives was also examined and the results are summarized in Table 2.

Laser flash photolysis was employed to elucidate the mechanistic details for photocatalytic chlorination. Transient absorption spectra taken after the nanosecond laser excitation at 430 nm of a degassed MeCN solution of $Acr^+–Mes$ in the absence and presence of TMB are shown in Fig. 7a. The absorption band due to the $Mes^{\bullet+}$

Table 2 One-electron oxidation potentials of substrates, products and quantum yields for photocatalytic chlorination of aromatic compounds by O_2 with HCl and Acr^+–Mes in O_2 saturated MeCN (conditions: [substrate] = 4.0 mM, [Acr^+–Mes ClO_4^-] = 0.20 mM, [HCl] = 20 mM)

Substrate	E_{ox} versus SCE (V)	Product	Conv. (%)	Yield (%)	Time (h)	Φ^a (%)
(anisole, OMe)	1.76	(4-chloroanisole, Cl–C6H4–OMe)	Trace		9	–
(1,3-dimethoxybenzene)	1.49	(chlorinated 1,3-dimethoxybenzene)	Trace		9	–
(1,3,5-trimethoxybenzene)	1.43	(chloro-1,3,5-trimethoxybenzene)	74	23	9	0.30
(1,2,4-trimethoxybenzene)	0.96	(chloro-1,2,4-trimethoxybenzene)	100	14	1.5	1.1

Photoirradiation by use of a xenon lamp attached with a color glass filter ($\lambda > 420$ nm)

[a] Φ was determined from the amount of the formation of chlorinated product

moiety ($\lambda_{max} = 500$ nm) of $Acr^•$–$Mes^{•+}$ was quenched by the addition of TMB. In the presence of TMB, a new absorption band at 450 nm appeared at 12 µs as shown in Fig. 7a, which is assigned to the TMB radical cation ($TMB^{•+}$) [64, 70]. The rate constant of electron transfer from TMB to the $Mes^{•+}$ of the electron-transfer state of Acr^+–Mes was determined from the slope of the linear plot of k_{rise} versus [TMB] to be $k_{TMB} = 2.0 \times 10^{10}$ M^{-1} s^{-1} [64]. The decay rate was accelerated with increasing concentration of HCl (Fig. 8a). The observed decay rate constant (k_{decay}) increases linearly with increasing concentration of HCl as shown in Fig. 8b. Thus, $TMB^{•+}$ efficiently reacts with Cl^- to form the Cl adduct radical [$TMB(Cl)^•$]. The rate constant for the addition of Cl^- to $TMB^{•+}$ was determined from the slope of k_{decay} versus [HCl] to be $k_{HCl} = 8.2 \times 10^7$ M^{-1} s^{-1} (Fig. 8b). The rate of electron-transfer oxidation of Cl^- in the photocatalytic reaction was also determined by quenching of the transient absorption of $Acr^•$–$Mes^{•+}$ by HCl to be 2.9×10^8 M^{-1} s^{-1} [39]. The lifetime of $TMB^{•+}$ is significantly longer than that of $Cl^•$ in MeCN under the photocatalytic conditions. Thus, the contribution of $Cl^•$ that is formed by the electron-transfer oxidation of Cl^- is negligible under the present reaction conditions.

The photocatalytic reaction is initiated by formation of intramolecular photoinduced electron transfer from the Mes moiety to the singlet excited state of the Acr^+ moiety of Acr^+–Mes to generate $Acr^•$–$Mes^{•+}$ as shown in Scheme 2. The electron-transfer state is stabilized as the π-dimer as mentioned in the previous section. The
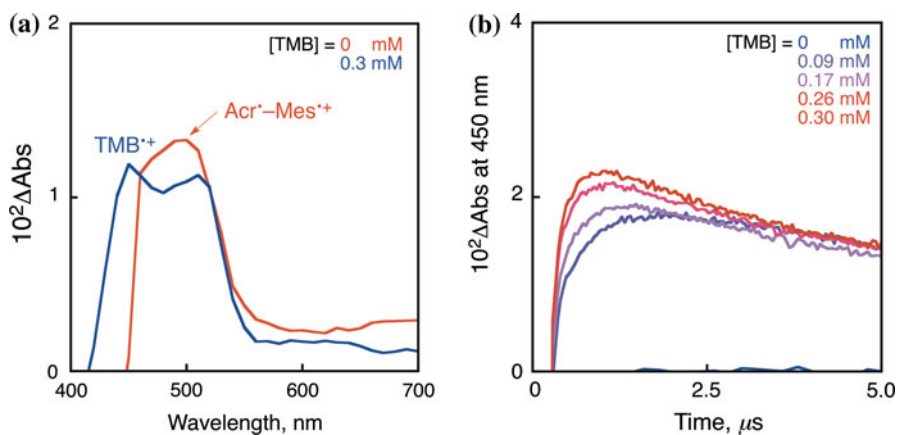
Fig. 7 **a** Transient absorption spectra for electron transfer from TMB (0–0.30 mM) to Acr$^{\bullet}$–Mes$^{\bullet+}$ in MeCN after nanosecond laser flash photolysis ($\lambda_{ex} = 430$ nm). **b** Transient absorbance time profiles at 450 nm due to TMB$^{\bullet+}$ observed in the presence of various concentration of TMB
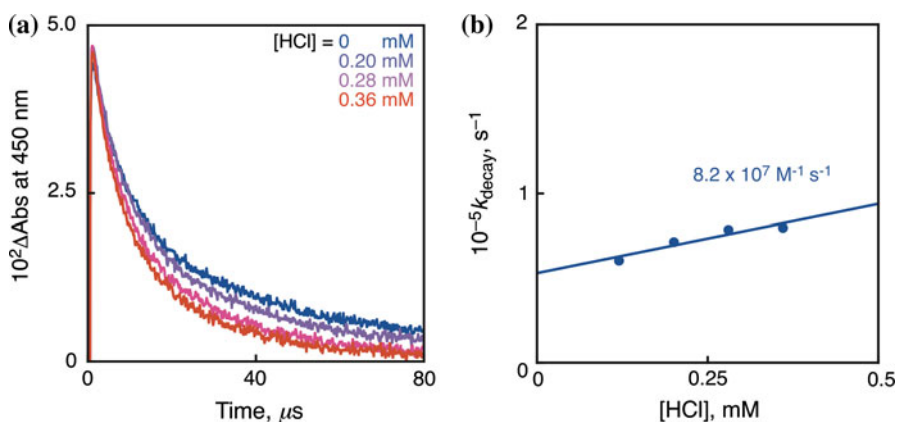

Fig. 8 **a** Transient absorbance time profiles at 450 nm. **b** Plot of k_{decay} versus [HCl] for the reaction of TMB$^{\bullet+}$ with HCl ($\lambda_{ex} = 430$ nm)

Mes$^{\bullet+}$ moiety can oxidize TMB to produce TMB$^{\bullet+}$, whereas the Acr$^{\bullet}$ moiety can reduce O$_2$ with proton to produce HO$_2^{\bullet}$. The TMB$^{\bullet+}$ thus produced reacts with Cl$^-$ to form the Cl adduct radical, which undergoes the dehydrogenation with HO$_2^{\bullet}$ to afford the corresponding chlorinated product and hydrogen peroxide. Hydrogen peroxide further reacts with HCl and substrate to produce another chlorinated product.

Conclusions

A donor–acceptor linked dyad, Acr$^+$–Mes, which has strong oxidizing and reducing abilities in the photoinduced electron-transfer state, has been shown to act as an efficient photocatalyst for the oxygenation of toluenes and chlorination of
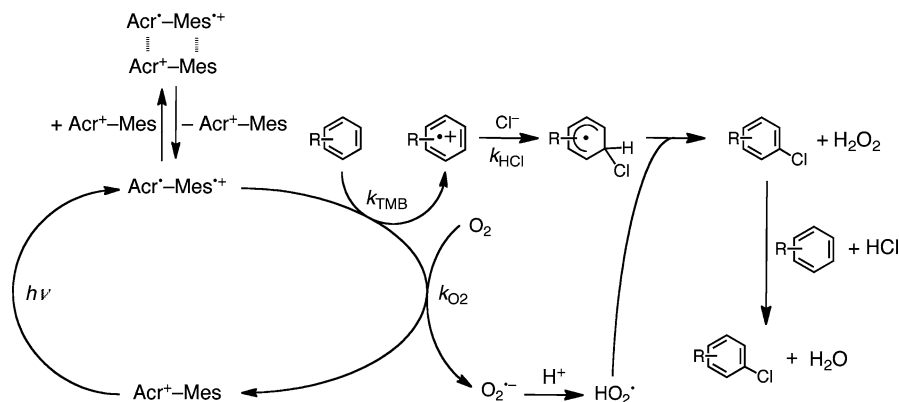
Scheme 2 Proposed catalytic reaction mechanism of photochlorination of aromatic hydrocarbon by Acr$^+$–Mes and HCl

methoxybenzenes with molecular oxygen as an oxidant. The radical intermediates in the photocatalytic oxidation and chlorination of substrates with O_2 were successfully detected by nanosecond transient absorption measurements to clarify the photocatalytic mechanisms.

References

1. R.C. Larock, *Comprehensive organic transformations: a guide to functional group preparations* (Wiley, New York, 1999)
2. I. Hermans, E.S. Spier, U. Neunschwanedr, N. Turrá, A. Baiker, Top. Catal. **52**, 1162–1174 (2009)
3. M.B. Smith (ed), in *March's Advanced Organic Chemistry*: *Reactions, Mechanisms, and Structure*, 6th edn. (Wiley, New York, 2007), pp. 698–705
4. R.C. Larock (ed), in *Comprehensive Organic Transformations*, 2nd edn. (Wiley, New York, 1999), pp. 622–624
5. A. Bottino, G. Capannelli, F. Cerutti, A. Comite, R. Di Felice, Chem. Eng. Res. Des. **82**, 229–235 (2004)
6. D. Dumitriu, R. Barjega, L. Frunza, D. Macovei, T. Hu, Y. Xie, V.I. Parvulescu, S. Kaliaguine, J. Catal. **219**, 337–351 (2003)
7. Y. Ishii, S. Sakaguchi, Catal. Surv. Jpn. **3**, 27–35 (1999)
8. R. Bandyopadhyay, S. Biswas, S. Guha, A.K. Mukherjee, R. Bhattacharyya, Chem. Commun. 1627–1628 (1999)
9. V.R. Durvasula, Synlett 495–496 (1992)
10. G. Barak, Y. Sasson, J. Chem. Soc., Chem. Commun. 637–638 (1988)
11. W. Bartok, D.D. Rosenfeld, A. Schriesheim, J. Org. Chem. **28**, 410–412 (1963)
12. R.A. Sheldon, J. Chem. Technol. Biotechnol. **68**, 381–388 (1997)
13. R.A. Sheldon, Chem. Ind. (London) 12–15 (1997)
14. T. Funabiki (ed) in *Oxygenases and Model Systems*. (Kluwer, Dordrecht, 1997)
15. D.H.R. Barton, A.E. Martell, D.T. Sawyer, *The activation of dioxygen and homogeneous catalytic oxidation* (Plenum, New York, 1993)
16. L.L. Simandi, *Dioxygen activation and homogeneous catalytic oxidation* (Elsevier, Amsterdam, 1991)

17. F. Müller, J. Mattay, Chem. Rev. **93**, 99–117 (1993)
18. J. Mattay, V. Martin, Top. Curr. Chem. **159**, 219–255 (1991)
19. M.A. Fox, M. Chanon (eds.), in *Photoinduced Electron Transfer*. (Elsevier, Amsterdam, 1988)
20. M. Julliard, M. Chanon, Chem. Rev. **83**, 425–506 (1983)
21. M. Julliard, C. Legris, M. Chanon, J. Photochem, Photobiol. A Chem. **61**, 137–152 (1991)
22. M. Julliard, A. Galadi, M. Chanon, J. Photochem. Photobiol. A Chem. **54**, 79–90 (1990)
23. L. Lopez, Top. Curr. Chem. **156**, 117–166 (1990)
24. A. Heumann, M. Chanon, in *Applied Homogeneous Catalysis with Organometallic Compounds*, ed. by B. Cornils, W.A. Herrmann (VCH, Weinheim, 1996), pp 929–948
25. W.P. Todd, J.P. Dinnocenzo, S. Farid, J.L. Goodman, I.R. Gould, J. Am. Chem. Soc. **113**, 3601–3602 (1991)
26. K. Ohkubo, K. Suga, K. Morikawa, S. Fukuzumi, J. Am. Chem. Soc. **125**, 12850–12859 (2003)
27. K. Suga, K. Ohkubo, S. Fukuzumi, J. Phys. Chem. A **109**, 10168–10175 (2005)
28. K. Ohkubo, K. Suga, S. Fukuzumi, Chem. Commun. 2018–2020 (2006)
29. K. Ohkubo, S. Fukuzumi, Org. Lett. **2**, 3647–3650 (2000)
30. K. Ohkubo, S. Fukuzumi, Bull. Chem. Soc. Jpn. **82**, 303–315 (2009)
31. S. Fukuzumi, H. Kotani, K. Ohkubo, S. Ogo, N.V. Tkachenko, H. Lemmetyinen, J. Am. Chem. Soc. **126**, 1600–1601 (2004)
32. K. Ohkubo, H. Kotani, S. Fukuzumi, Chem. Commun. 4520–4522 (2005)
33. K. Ohkubo, K. Mizushima, R. Iwata, K. Souma, N. Suzuki, S. Fukuzumi, Chem. Commun. **46**, 601–603 (2010)
34. S. Fukuzumi, K. Ohkubo, T. Suenobu, K. Kato, M. Fujitsuka, O. Ito, J. Am. Chem. Soc. **123**, 8459–8467 (2001)
35. R.D. Mair, A.J. Graupner, Anal. Chem. **36**, 194–204 (1964)
36. S. Fukuzumi, S. Kuroda, T. Tanaka, J. Am. Chem. Soc. **107**, 3020–3027 (1985)
37. S. Fukuzumi, M. Ishikawa, T. Tanaka, J. Chem. Soc. Perkin Trans. 2, 1037–1045 (1989)
38. C.G. Hatchard, C.A. Parker, Proc. R. Soc. London Ser. A **235**, 518–536 (1956)
39. K. Ohkubo, A. Fujimoto, S. Fukuzumi, Chem. Commun. **47**, 8515–8517 (2011)
40. A.C. Benniston, K.J. Elliott, R.W. Harrington, W. Clegg, Eur. J. Org. Chem. **2**, 253–258 (2009)
41. A.C. Benniston, A. Harriman, P. Li, J.P. Rostron, J.W. Verhoeven, Chem. Commun. 2701–2703 (2005)
42. A.C. Benniston, A. Harriman, P. Li, J.P. Rostron, H.J. van Ramesdonk, M.M. Groeneveld, H. Zhang, J.W. Verhoeven, J. Am. Chem. Soc. **127**, 16054–16064 (2005)
43. A.C. Benniston, A. Harriman, J.W. Verhoeven, Phys. Chem. Chem. Phys. **10**, 5156–5158 (2008)
44. H. van Willigen, G. Jones II, M.S. Farahat, J. Phys. Chem. **100**, 3312–3316 (1996)
45. S. Fukuzumi, H. Kotani, K. Ohkubo, Phys. Chem. Chem. Phys. **10**, 5159–5162 (2008)
46. S. Fukuzumi, R. Hanazaki, H. Kotani, K. Ohkubo, J. Am. Chem. Soc. **132**, 11002–11003 (2010)
47. Y. Yamada, T. Miyahigashi, H. Kotani, K. Ohkubo, S. Fukuzumi, J. Am. Chem. Soc. **133**, 16136–16145 (2011)
48. H. Kotani, K. Ohkubo, S. Fukuzumi, Faraday Disccuss. **155**, 89–102 (2012)
49. O. Morawski, J. Prochorow, Chem. Phys. Lett. **242**, 253–258 (1995)
50. K. Kikuchi, C. Sato, M. Watabe, H. Ikeda, Y. Takahashi, T. Miyashi, J. Am. Chem. Soc. **115**, 5180–5184 (1993)
51. K. Kasama, K. Kikuchi, Y. Nishida, H. Kokubun, J. Phys. Chem. **85**, 4148–4153 (1981)
52. H. Kotani, K. Ohkubo, S. Fukuzumi, J. Am. Chem. Soc. **126**, 15999–16006 (2004)
53. K. Ohkubo, T. Nanjo, S. Fukuzumi, Org. Lett. **7**, 4265–4268 (2005)
54. K. Ohkubo, T. Nanjo, S. Fukuzumi, Catal. Today **117**, 356–361 (2006)
55. K. Ohkubo, K. Yukimoto, S. Fukuzumi, Chem. Commun. 2504–2506 (2006)
56. K. Ohkubo, T. Nanjo, S. Fukuzumi, Bull. Chem. Soc. Jpn. **79**, 1489–1500 (2006)
57. S. Fukuzumi, Bull. Chem. Soc. Jpn. **79**, 177–195 (2006)
58. H. Kotani, K. Ohkubo, Y. Takai, S. Fukuzumi, J. Phys. Chem. B **110**, 24047–24053 (2006)
59. H. Kotani, T. Ono, K. Ohkubo, S. Fukuzumi, Phys. Chem. Chem. Phys. **9**, 1487–1492 (2007)
60. K. Ohkubo, R. Iwata, T. Yanagimoto, S. Fukuzumi, Chem. Commun. 3139–3141 (2007)
61. H. Kotani, K. Ohkubo, S. Fukuzumi, Appl. Catal. B Environ. **77**, 317–324 (2008)
62. S. Fukuzumi, Eur. J. Inorg. Chem. 1351–1362 (2008)
63. S. Fukuzumi, Phys. Chem. Chem. Phys. **10**, 2283–2297 (2008)
64. K. Ohkubo, K. Mizushima, R. Iwata, S. Fukuzumi, Chem. Sci. **2**, 715–722 (2011)

65. S. Fukuzumi, Y. Yamada, T. Suenobu, K. Ohkubo, H. Kotani, Energy Environ. Sci. **4**, 2754–2766 (2011)
66. K. Ohkubo, R. Iwata, S. Miyazaki, T. Kojima, S. Fukuzumi, Org. Lett. **8**, 6079–6082 (2006)
67. M. Tanaka, K. Ohkubo, C.P. Gros, R. Guilard, S. Fukuzumi, J. Am. Chem. Soc. **128**, 14625–14633 (2006)
68. M. Murakami, K. Ohkubo, T. Nanjo, K. Souma, N. Suzuki, S. Fukuzumi, Chem. Phys. Chem. **11**, 2594–2605 (2010)
69. M. Murakami, K. Ohkubo, S. Fukuzumi, Chem. Eur. J. **16**, 7820–7832 (2010)
70. T. Shida, *Electronic absorption spectra of radical ions* (Elsevier, Amsterdam, 1988)